JOC The Journal of Organic Chemistry

Article

Deoxynucleoside Triphosphate Containing Pyridazin-3-one Aglycon as a Thymidine Triphosphate Substitute for Primer Extension and Chain Elongation by Klenow fragments

Takahito Tomori, Kento Nagaoka, Leo Takeshita, Takashi Shiozawa, Yuya Miyatake, Yoshiaki Masaki, Mitsuo Sekine, and Kohji Seio

J. Org. Chem., **Just Accepted Manuscript** • DOI: 10.1021/acs.joc.8b00918 • Publication Date (Web): 28 Jun 2018

ACS Publications

is published by the American Chemical Society. 1155 Sixteenth Street N.W., Washington, DC 20036

Deoxynucleoside Triphosphate Containing Pyridazin-3-one Aglycon as a Thymidine Triphosphate Substitute for Primer Extension and Chain Elongation by Klenow Fragments

Takahito Tomori, Kento Nagaoka, Leo Takeshita, Takashi Shiozawa, Yuya Miyatake, Yoshiaki Masaki, Mitsuo Sekine, and Kohji Seio*

School of Life Science and Technology, Tokyo Institute of Technology, 4259 Nagatsuta, Midoriku, Yokohama, 226-8501, Japan

kseio@bio.titech.ac.jp

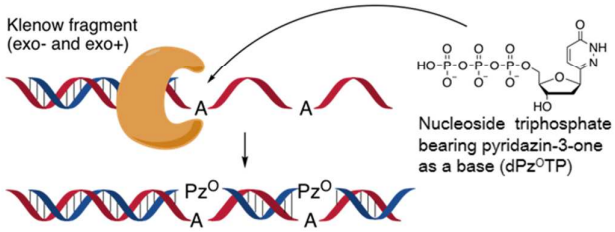

Abstract

Deoxynucleoside 5'-triphosphate was synthesized with 3-oxo-2*H*-pyridazin-6-yl (Pz^O)—a uracil analog lacking a 2-keto group—as the nucleobase. Theoretical analyses and hybridization experiments indicated that Pz^O recognizes adenine (A) for formation of a Watson-Crick base pair. Primer extension reactions using nucleoside 5'-triphosphate and Klenow fragment revealed that the synthetic nucleoside 5'-triphosphate was incorporated into the 3' end of the primer through recognition of A in the template strand. Moreover, the 3'-nucleotide residue harboring Pz^O as the base was resistant to the 3'-exonuclease activity of Klenow fragment exo+. The primer bearing the Pz^O base at the 3' end could function in subsequent chain elongation. These properties of Pz^O were attributed to the presence of an endocyclic nitrogen atom at the position ortho to the glycosidic bond, which was presumed to form an H-bond with the amino acid residue of DNA polymerase for effective recognition of the 3' end of the primer for primer extension. These results provide a basis for designing new nucleobases by combining a nitrogen atom at the position ortho to the glycosidic bond and base-pairing sites for Watson-Crick hydrogen bonding.

Introduction

The development of deoxynucleotides bearing unnatural nucleobases that can be introduced into genomic DNA by DNA polymerases[1,2,3] has been widely studied in the field of synthetic biology. To this end, many types of unnatural base pairs including NaM-5SICS,[4,5] Ds-Pn(x),[6,7] and P-Z[8] have been synthesized. Artificial nucleobases must have several features for incorporation into genomic DNA. Firstly, the artificial deoxynucleoside 5'-triphosphate must be capable of incorporation into the 3' terminal hydroxyl group of the primer recognizing the counter nucleobase on the template. Secondly, the primer bearing the artificial nucleoside residue at the 3' end must be amenable to extension by DNA polymerases. Thirdly, the artificial nucleotide at the 3' end of the primer must be resistant to the proofreading 3'→5' exonuclease activity DNA polymerases.

To meet the first criterion, artificial base pairs recognizing counter bases either through hydrogen bonding[8] or shape fitting[4,5,6,7,9] have been developed. For the second criterion, an H-bond acceptor on the minor groove side of nucleobases—referred to as the minor groove H-bond acceptor—is required. In the case of the natural nucleobases, the nitrogen at position 3 (N3) and 2-keto group of purine and pyrimidine nucleobases, respectively, function as minor groove H-bond acceptors. Their importance has been supported by X-ray crystallographic studies[10-12] of binary complexes consisting of DNA polymerase and a primer-template duplex, or of ternary complexes containing an additional nucleoside triphosphate. For example, in the binary complex consisting of *Thermus aquaticus* (*Taq*) DNA polymerase I—a DNA polymerase belonging to the A family—and a primer-template duplex, Arg573 of the polymerase recognized nucleobases at the 3' end of the primer, at the N3 of guanine (G) or 2-keto of cytosine (C).[11] The same crystallographic structures also demonstrated the recognition of the 2-keto of C or the N3 of G in the corresponding position in the template by Gln754. In fact, successful artificial base pairs have minor groove H-bond acceptors. For example, the NaM-5SICS pair has a methoxy group in NaM and a thioketo group in 5SICS; the Ds-Pn pair has an endocyclic nitrogen atom in Ds and a nitro group in Pn; and the P-Z pair has an endocyclic nitrogen in P and keto group in Z. X-ray crystallographic studies of these artificial base pairs have revealed the expected H-bonding in the minor groove.[10, 13]

Various heteroaromatic groups harboring an endocylic nitrogen or oxygen atom at the position *ortho* to the glycosidic bond have been reported as a potential scaffold for new artificial nucleobase analogs bearing a minor groove H-bond acceptor, including benzofuran-2-yl or benzotriazol-2-yl[14] and pyridine-2-yl (2Py).[15] An investigation of the DNA polymerase reaction using a primer-template duplex containing a 2Py residue at both 3' ends of the primer and at the counter position of the template as a 2Py-2Py self-pair[15] found that strand extension catalyzed by Klenow fragment exo- (Kf−) proceeded more rapidly from the primer harboring 2Py than from the primer-template duplex containing other pairs of six-membered rings without a nitrogen atom at the position *ortho* to the glycosidic bond. These results suggest that this nitrogen atom acts as a minor groove H-bond

acceptor. However, 2Py itself has not been used for artificial self-pairing because it can accommodate dATP or dGTP more efficiently when incorporated into the template strand. Therefore, if the 2Py structure is used as the scaffold for artificial nucleobases, some functional groups must be introduced that recognize specific nucleobase analogs via appropriate noncovalent interactions such as hydrogen bonds.

Based on these considerations, we designed pyridazin-3-one (Pz^O; Figure 1a) as a new artificial nucleobase. Pz^O was designed with H-bonding sites to form Watson-Crick base pairs with A, including a carbonyl group at position 3 and an imino group at position 2. It also has a nitrogen atom at position 2 as the minor groove H-bond acceptor in the case of 2Py (Figure 1a). Since Pz^O was designed to recognize the natural nucleobase A, it cannot itself be a component of new artificial pairs. The aim of this study was to demonstrate that the combination of nitrogen at the *ortho* position and hydrogen sites for base pairing is an effective design strategy for artificial bases.

We synthesized a deoxynucleoside triphosphate (**1**) with Pz^O as an aglycon (Figure 1b), and characterized its properties including base-pairing stability and selectivity by preparing DNA duplexes in which Pz^O was incorporated using phosphoramidite (**2**) (Figure 1b). Additionally, we examined reactions catalyzed by Kf− and Klenow fragment exo+ (Kf+) using **1** instead of thymidine 5'-triphosphate (TTP). Our results show that Pz^O can selectively recognize A during DNA duplex formation and enzymatic base incorporation. In addition, the primer harboring Pz^O at the 3' end could be elongated by either Kf− or Kf+, despite the absence of the 2-keto carbonyl group.

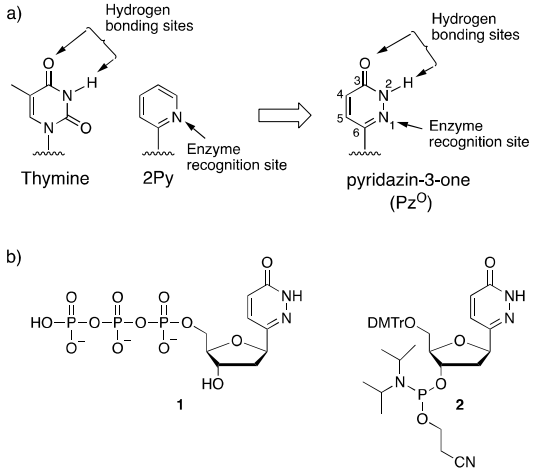

Figure 1. a) Design and structure of a pyridazine-type nucleobase (Pz^O) with sites for hydrogen bonding with A and an enzyme recognition site. b) Structure of **1** and **2**.

Results and Discussion

Hydrogen bond properties of Pz^O

The hydrogen bond energies between Pz^O or thymine (T) and A or G were calculated according to the density functional theory of electronic structure at the M06-2X/6-311+G(2df,p)//M06-2X/6-31+G(d,p) level (Figure 2).[16] In this calculation, we used 6-methylpyridazin-3-one, 1-methylthymine, 9-methyladenine, and 9-methylguanine as model structures for Pz^O, T, A, and G, respectively. Base-pairing energies were calculated as energy differences between X-Y complexes such as A-T, G-T, A-Pz^O, and G-Pz^O, and the sum of each base. The basis set superposition error was estimated using the counterpoise method.[17] Base pair structures and base-pairing energies are shown in Figure 2. Pz^O formed base pairs with A in the Watson-Crick geometry (Figure 2a). The base-pairing energy for the A-Pz^O pair was −13.8 kcal/mol, which was almost identical to that of the A-T base pair (−13.7 kcal/mol) (Figure 2b). These results suggest that the A-Pz^O base pairing is as stable as A-T.

We also calculated the base-pairing energy of G-Pz^O (Figure 2c) and G-T (Figure 2d) pairs starting from wobble geometry. The value of the G-Pz^O pair was −10.9 kcal/mol, which was larger than that of G-T base pair (−14.6 kcal). The lower stability of the G-Pz^O base pair can be explained by two factors. Firstly, although two hydrogen bonds were formed in both base pairs, the absence of a 2-keto group in Pz^O shortened the distance between the 2-amino group of G and the methyl group corresponding to the C1' position of Pz^O. Consequently, the planes of Pz^O and G were twisted by 14.3° while T and G were co-planar (Figure S1), which prevented steric clashing between the methyl and amino groups. Secondly, as indicated by the electrostatic potential map of Pz^O (Figure 3a) and T (Figure 3b), the N1 of Pz^O was less negative than the 2-keto group of T. Thus, hydrogen bonding between the N1 of Pz^O and the amino group of G may be intrinsically weaker than that between the 2-keto of T and the amino group of G.

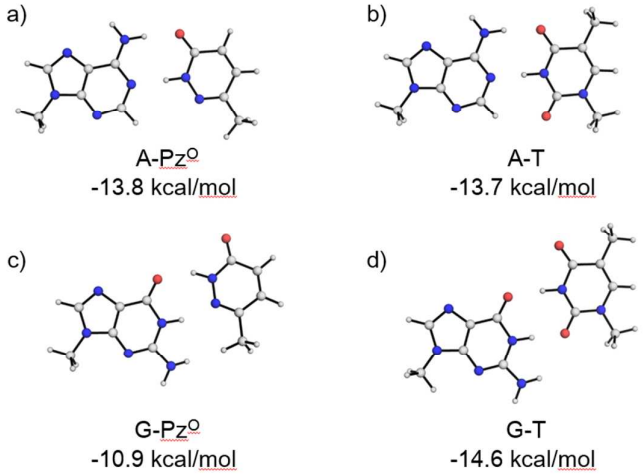

Figure 2. Base-pair structures and energies of a) A-Pz^{O}, b) A-T, c) G-Pz^{O}, and d) G-T.

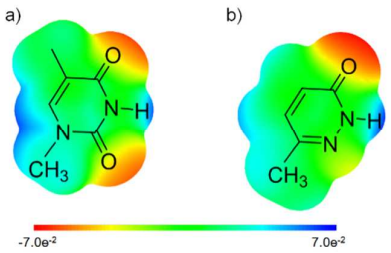

Figure 3. Electrostatic potential of electron density from total self-consistent field density (isovalue = 0.001) of a) T and b) Pz^{O}. The color bar indicates electrostatic potential from $-7.0e^{-2}$ to $7.0e^{-2}$. Images were generated with GaussView v.6.0.16. Chemical structures were overlaid to show the approximate positions of atoms.

Synthesis of ribonucleoside, deoxynucleoside, triphosphate, and phosphoramidite harboring Pz^{O} as a nucleobase

We synthesized the nucleoside triphosphate **1** and phosphoramidite **2**. Although methods for synthesizing a *C*-nucleosides from a glycal and a heteroaromatic compound using transition metal catalyst has been reported so far, the pyridazin deravatives have never been introduced by these methods.[18,19] Indeed, we applied these method using 3,6-dibromopyiridazon, but the *C*-glycosidic bond did not form (data not shown). Therefore, we carried out the synthesis of ribonucleoside **10**[20,21] and deoxynucleoside **13** (dPz^{O})[22] with Pz^{O} as the base moiety by optimizing previously reported procedure. The compounds were synthesized via known intermediates **4**,[23] **5**,[20,21,22] **6**,[21] and **9**,[21] but the conditions and routes of synthesis were modified for maximal yield.

The new synthetic route for synthesis of dPz^{O}TP (**1**) and phosphoramidite derivatives (**2**) is outlines in Scheme 1.

We first synthesized compound **4**[23] from **3** by Friedel-Crafts *C*-glycosilation catalyzed by $SnCl_4$. Under the previously reported conditions,[23] the major product was a compound with two furan rings at position 1 of the ring-opened ribose skeleton. This per-furanylation was suppressed when the amount of $SnCl_4$ was reduced from 1.1 to 0.1 equiv. The acetyl groups of **4** were removed by sodium methoxide; re-protection with benzoyl groups yielded **5**, which had increased lipophilicity. Oxidation of compound **5** produced **6**, which was converted to compound **7** by hydrogenation. We used 4-(4,6-dimethoxy-1,3,5-triazin-2-yl)-4-methylmorpholinium chloride as the condensing agent in the cyclization of **7** to **8** using hydrazine, and **8** was then converted to **10** via oxidization by 2,3-dichloro-5,6-dicyanobenzoquinone[22] and deprotection by treatment with 28% aqueous NH_3.

We next synthesized deoxynucleoside derivatives from ribonucleoside **10**. The 3' and 5' hydroxyl groups were protected with 1,1,3,3-tetraisopropyldisiloxane-1,3-diyl to obtain **11**, which was deoxygenated by treatment with *O*-phenyl chlorothionoformate followed by reduction using

Tris(trimethylsilyl)silane and azobisisobutyronitrile as reducing agent and radical initiator, respectively. The resultant compound **12** was deprotected using triethylamine-tris(hydrogen fluoride) to obtain the deoxynucleoside **13** (73% yield). Compound **13** was converted to the triphosphate derivative **1** in three steps (27% yield) using phosphoryl chloride and pyrophosphate,[24,25] and then separated on a diethyl-aminoethyl Sephadex A-25 column (Figures S2 and S3). The phosphoramidite derivative **2** was also synthesized. The 5'-hydroxyl group was protected by 4, 4' dimethoxytrityl to obtain **14** (53% yield), which was phosphitylated to obtain **2** (50% yield). The structures of the synthesized compounds were characterized by ^{1}H- and other types of nuclear magnetic resonance spectroscopy (see the Supporting Information) and by electrospray ionization (ESI) time-of-flight (TOF) mass spectrometry (MS).

Scheme 1. Synthesis of dPz^{O} triphosphate (**1**) and phosphoramidite derivatives (**2**).

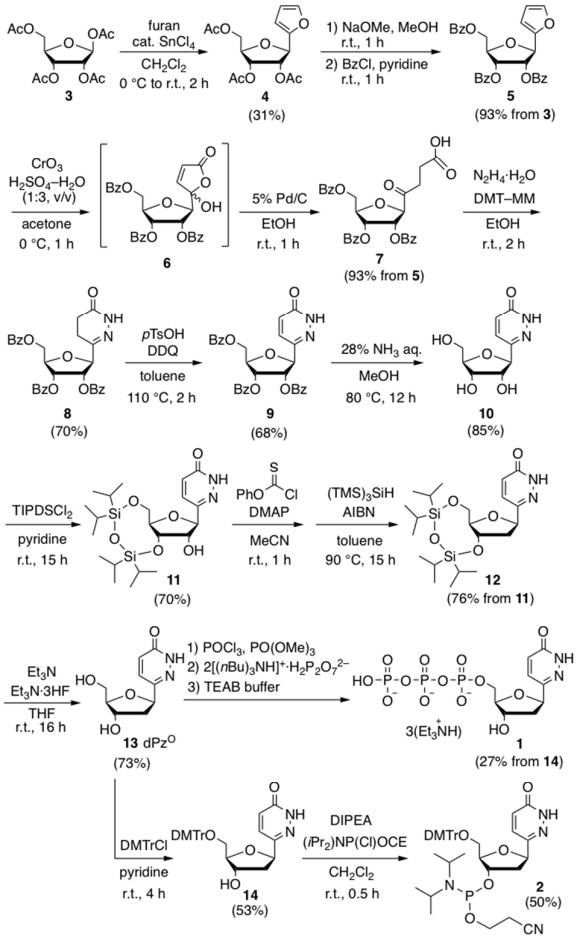

Oligodeoxynucleotide (ODN) synthesis and ultraviolet (UV) melting curve analysis

To investigate the base-pairing capacity of Pz^O, the hybridization properties of ODNs containing Pz^O were examined by measuring the melting temperature (T_m) of ODN duplexes modified with Pz^O and their complementary and non-complementary ODNs. The ODNs were synthesized according to the standard phosphoramidite method on an automated DNA synthesizer without modifications. The sequences of the synthesized and purchased ODNs are shown in Figure 4a. **ODN1** had Pz^O incorporated at the position indicated by [X], and was synthesized from **2** and commercially available deoxynucleoside phosphoramidites. The ODNs were purified by anion exchange high-performance liquid chromatography and characterized by matrix-assisted laser desorption/ionization-TOF MS (Figures S4 and S5).

ODN2 was synthesized as an unmodified ODN containing T instead of Pz^O. The sequence of **cODN1** was complementary to that of **ODN2**, with an A at the position indicated by [Y]. **cODN2–4** were mismatched sequences with G, C, and T, respectively, at the [Y] position.

a) Oligonucleotides for T_m measurements

5′GCGTAC [X] CATGCG3′
ODN1: X = Pz^O, ODN2: X = T

3′CGCATG [Y] GTACGC5′
cODN1: Y = A, **cODN2**: Y = G
cODN3: Y = C, **cODN4**: Y = T

b) Primer and 25nt templates

FAM-5′CGCGCGAAGACCGGTTAC3′
P1

3′GCGCGCTTCTGGCCAATG [Z] CTGTCT5′
T1: Z = A, **T2**: Z = G
T3: Z = C, **T4**: Z = T

c) 30nt templates

T5 3′GCGCGCTTCTGGCCAATG A CTGTCTGCTTC5′
T6 3′GCGCGCTTCTGGCCAATG AA TGTCTGCTTC5′
T7 3′GCGCGCTTCTGGCCAATG ACA GTCTGCTTC5′
T8 3′GCGCGCTTCTGGCCAATG ACTA TCTGCTTC5′
T9 3′GCGCGCTTCTGGCCAATG ACTGA CTGCTTC5′
T10 3′GCGCGCTTCTGGCCAATG ACTGTA TGCTTC5′

d) Synthetic control sequences

P2 FAM-5′CGCGCGAAGACCGGTTACT3′ (19-nt)
P3 FAM-5′CGCGCGAAGACCGGTTACTGACAGA3′(25-nt)
P4 FAM-5′CGCGCGAAGACCGGTTACTGACAGACGAAG3′ (30-nt)

e) Expected products

P5 FAM-5′CGCGCGAAGACCGGTTACT Pz^O GAC3′

Figure 4. a) Sequences of ODNs used in hybridization studies. b) Sequences of primers and 25-nt templates used in single nucleotide insertion and full-length primer extension studies. c) Sequences of 30-nt templates used in the chain elongation reaction. d) Sequences of size markers used in PAGE analyses.

The T_m values of duplexes formed between **ODN1** or **ODN2** and **cODN1–4** were determined from UV melting curves (Figures S6 to S9) and are summarized in Table 1. The T_m of **ODN1** and

cODN1 was 54.3°C, which was 3.5°C lower than that of the **ODN2/cODN1** duplex (T_m = 57.8°C). The higher T_m of the latter may reflect the stacking effects of the methyl and keto groups at positions 5 and 2, respectively, of the T at position [X], which stabilized the duplex. On the other hand, the T_m values of mismatched duplexes containing **ODN1** and **ODN2** were 27.4°C and 31.3°C, respectively, for the duplex with **cODN2**; 40.2°C and 41.2°C, respectively, for the duplex with c**ODN3**; and 45.2°C and 48.3°C, respectively, for the duplex with **cODN4**. Base recognition by Pz^O and T were compared according to differences in T_m values between matched duplexes (e.g., **ODN1**/**cODN1** and **ODN2**/**cODN1**) and the most stable mismatched duplexes (e.g., **ODN1**/**cODN4** and **ODN2**/**cODN4**). The base recognition capacities of **ODN1** and **ODN2** were nearly identical (−9.1°C vs. –9.5°C).

Table 1. Base recognition capacity of Pz^O

ODN (X)	**cODN** (Y)	T_m[a]/°C	ΔT_m[b]/°C
ODN1 (X = Pz^O)	**cODN1** (Y = A)	54.3 (0.25)	−
	cODN2 (Y = G)	27.4 (0.98)	−26.9
	cODN3 (Y = C)	40.2 (0.25)	−14.1
	cODN4 (Y = T)	45.2 (0.11)	−9.1
ODN2 (X = T)	**cODN1** (Y = A)	57.8 (0.49)	−
	cODN2 (Y = G)	31.3 (0.25)	−26.5
	cODN3 (Y = C)	41.2 (0.25)	−16.6
	cODN4 (Y = T)	48.3 (0.24)	−9.5

[a] T_m values (and standard deviations in parentheses) were measured in 10 mM sodium phosphate (pH 7.0) containing 0.1 M NaCl, 0.1 mM EDTA, and 2.0 μM each ODN.

[b] $\Delta T_m = T_m - T_m$ (Y = A)

Single nucleotide insertion by Kf−

To investigate the template-specific incorporation of **1** by DNA polymerase, we examined single nucleotide insertion using the Kf− of *Escherichia coli* DNA polymerase lacking 3' to 5' exonuclease activity. Template and primer sequences are shown in Figure 4b. The templates **T1**, **T2**, **T3**, and **T4** were single stranded 25-nt ODNs containing A, G, C, and T, respectively, at position [Z]. Primer **P1** was a single-stranded 18-nt DNA whose 5' end was labeled with a carboxyfluorescein residue (FAM in Figure 4b). One of **T1** to **T4** along with **P1**, and 10 μM of **1** or 10 μM TTP was incubated in the presence of Kf− for single nucleotide incorporation (Figure 5a). The reaction products were analyzed by 20% polyacrylamide gel electrophoresis (PAGE) containing 7 M urea (Figure 5b). Lane 1 shows the band corresponding to **P1**; lanes 2–5 are for experiments using **1** and **T1**–**T4**, in which A, G, C, and T, respectively, occupied position [Z] of the template; lanes 6–9 are for experiments using TTP and **T1**–**T4**, respectively. Shown in lane 10 is the synthetic 19-nt control (**P2** in Figure 4d), whose sequence was identical to **P1** but with an additional T residue at the 3' end. Compound **1** was incorporated when [Z] was A (lane 2) but not when it was G, C, or T (lanes 3–5). Under these conditions, TTP was incorporated when [Z] = A (lane 6), but minor band corresponding to the 19-nt product was observed even when [Z] = G, C, and T (lanes 7–9), because the TTP concentration was higher than the K_m of the Kf−-catalyzed TTP incorporation reaction (discussed below). Thus, 10 μM **1** was predominantly incorporated into the site opposite to A without giving mis-incorporated products.

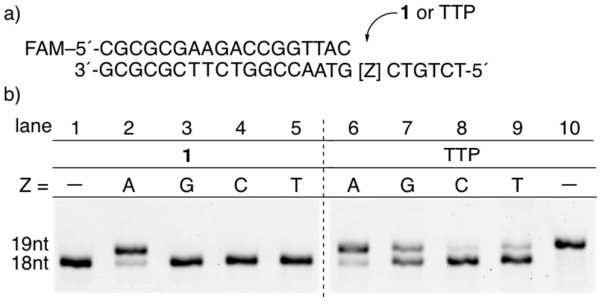

Figure 5. PAGE analysis of single nucleotide incorporation of **1** or TTP into **P1** in the presence of 25-nt **T1**–**T4**. Lanes 1 and 10 correspond to the synthetic 18-nt primer **P1** and 19-nt synthetic control **P2**, respectively. Conditions: 0.1 μM template (**T1**–**T4**); 0.1 μM **P1**; 10 μM each TTP or **1**; 0.01 U/μl Kf−; and reaction time = 10 min.

To determine the incorporation efficiency of **1**, we evaluated the steady-state kinetic parameters for the single nucleotide insertion reaction using Kf− (Table 2). The K_m, V_{max}, and V_{max}/K_m values were determined using **T1** as the template. The K_m values for **1** and TTP were 9 and 0.07 μM, respectively. On the other hand, **1** and TTP had nearly identical V_{max} values (21%·and 25%·min^{-1}, respectively). The large K_m of **1** indicated that the affinity of **1** for the binary complex

consisting of Kf− and the **P1**/**T1** duplex was roughly two orders of magnitude lower than that of TTP. On the other hand, the similar V_{max} values of **1** and TTP indicated that the kinetics of phosphodiester bond formation in the ternary complex consisting of Kf−, **1**, and the **P1**/**T1** duplex were as rapid as those in the complex with TTP instead of **1**. Accordingly, the gross reaction efficiency as evaluated by V_{max}/K_m was 2.9×10^8 and 2.8×10^6 for TTP and **1**, respectively, indicating that **1** was incorporated about 100 times less efficiently than TTP.

Table 2. Steady-state kinetic parameters for the insertion of a single dNTP into a **P1**/**T1** duplex by Kf−

N	K_m (μM)	V_{max} (%·min^{-1})	V_{max}/K_m (%·min^{-1}·M^{-1})
T	0.07 (0.02)	21 (4.0)	2.9 x 10^8
Pz^O	9.0 (0.9)	25 (4.0)	2.8 x 10^6

Full-length primer extension by Kf−

We performed the full-length extension of **P1** using **T1**, Kf−, and a mixture of dATP, dGTP, and dCTP in the presence or absence of **1** or TTP (Figure 6). The band in lane 1 corresponds to **P1**, and lane 5 shows the synthetic 25-nt **P3** (Figure 4c) with a chain length identical to that of the expected full-length product. Lane 2, which is the reaction product in the absence of **1** or TTP, had a thin band corresponding to the 19-nt product generated by incorporation of dGTP, dCTP, or dATP mismatched with A.

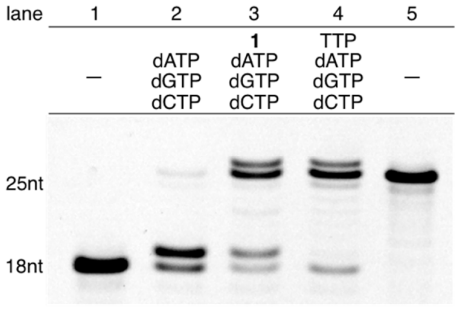

Figure 6. Full-length primer extension by Kf− using **P1** and **T1** by. Lane 1, **P1**: lane 2, reaction in the presence of dATP, dGTP, and dCTP; lane 3, reaction in the presence of **1**, dATP, dGTP, and dCTP; lane 4, reaction in the presence of TTP, dATP, dGTP, and dCTP; lane 5, 25-nt control **P3**. Conditions: 0.1 μM **T1**, 0.1 μM **P1**, 10 μM each dNTP, 0.01 U/μl Kf−, and reaction time = 10 min.

The reaction in the presence of **1**, dGTP, dCTP, and dATP (lane 3) yielded a products that appeared at the same position as the synthetic 25-nt control **P3** (lane 5) and 26-nt product. The mobility of these bands were also identical to those of the band in lane 4, in which TTP was used

instead of **1**. These results indicate that **1** was incorporated into the position opposite A without disrupting subsequent chain elongation, resulting in a full-length product.

Incorporation of 1 by Kf− at two positions

To further evaluate the properties of **1**, we used a duplex consisting of **P1** and the 30-nt template **T9** (Figure 4c) containing two A residues flanking the 5'-CGT-3' trinucleotide sequence in the single-stranded region of the primer-template duplex (Figure 7). Shown in lane 1 is the band corresponding to **P1**; lanes 7 and 14 show the synthetic control **P4** (Figure 4d), whose chain length was 30-nt. When 10 μM **1** was used (left panel), an intermediate product (*) presumed to be **P5** (Figure 4f) was observed at 5–60 min. On the other hand, the expected full-length products at the position close to that of the synthetic control **P4** (lanes 7 and 14) were not observed in lanes 2 and 3 at 5 and 10 min. The amount of full-length product increased over time (lanes 4–6), becoming the main band after 60 min (lane 6). It is worth noting that in these experiments, the full-length product comprised 31-nt ODNs that were longer than the synthetic control **P4** by one nucleotide, as determined based on gel mobility. The sequence of the full-length product was likely 31 nt with one of the four nucleotide residues at the 3′ end resulting from the template-independent incorporation activity of Kf–.[26]

The same experiments carried out at 100 μM **1** (right panel) showed that the full-length product was obtained as the major product within 30 min (lane 10).

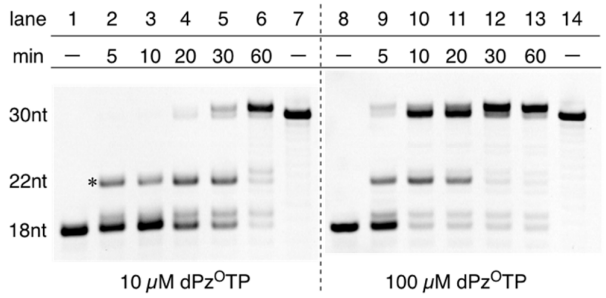

Figure 7. Time course of full-length primer extension with incorporation of two dPz^{O} residues. Lane 1, **P1**; lanes 2–6, time course of reaction in the presence of 10 μM **1**; lane 7, 30-nt synthetic control **P4**; lane 8, **P1**; lanes 9–13, time course of reaction in the presence of 100 μM **1**; lane 14, 30-nt synthetic control **P4**. Conditions: 0.1 μM **T9**; 0.1 μM **P1**; 10 μM dATP, dGTP, and dCTP; 0.01 U/μl Kf−.

To further evaluate the properties of **1** in the chain elongation reactions, we used templates **T5** and **T6**–**T10** (Figure 4c), incorporating two consecutive A residues or two A residues flanking one to four nucleotides. The chain elongation reactions were carried out in the presence of 100 μM **1** (Figure 8). Lane 1 corresponds to **P1**; lane 2 represents the reaction with **P1**, **T5**, dGTP, dATP, and

dCTP; lanes 3–8 corresponded to the reaction of **P1** and **T5**–**T10** in the presence of dGTP, dATP, dCTP, and **1**; and lane 10 shows the reaction of **P1** and **T5** in the presence of the four canonical deoxynucleoside triphosphates. As shown by PAGE, chain elongation was terminated only in the reaction shown in lane 4 that used template **T6** containing two consecutive A residues. The position of the band was the same as that observed in lane 2, in which neither TTP nor **1** was included and chain elongation was halted after incorporation of a mismatched nucleotide. In contrast, the full-length products were observed in lanes 5–8. Thus, once **1** was incorporated at the first position, a second **1** could also be incorporated by Kf− as long as the template was designed so that two A residues were not arranged consecutively. The reason for the failure of consecutive incorporation is unclear. However, the X-ray crystallographic studies revealed that the nucleobases of dNTP and the 3' ends of the primer were well stacked in the ternary complex consisting of DNA polymerase, primer-template duplex, and dNTP,[27] thus, the second **1** may not be properly fixed at the 3' end of the primer when there is a weak stacking interaction between two Pz^O residues which lack 5-methyl and 2-keto groups.

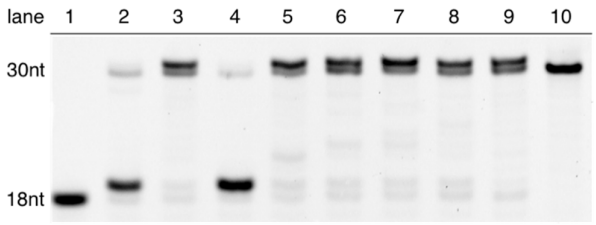

Figure 8. Incorporation of one (lane 3) or two (lanes 4–8) dPz^O residues at various positions. Lane 1, **P1**; lane 2, reaction in the presence of **P1**, **T5**, dATP, dGTP, and dCTP; lane 3, conditions for lane 2 plus **1**; lanes 4–8, reaction using **T6**–**T10**; lane 9, conditions for lane 2 plus TTP; lane 10, **P4**. Conditions: 0.1 μM template; 0.1 M **P1**; 10 μM dATP, dGTP, TTP, and dCTP; 100 μM **1**; 0.01 U/μl KF−; and reaction time = 60 min.

Single nucleotide and full-length primer extension by Kf+

We evaluated the properties of **1** as a substrate of Kf+—which possesses 3' to 5' exonuclease activity—by performing the single nucleotide extension reaction using primer **P1** and the 25-nt template **T5** (Figure 9). As seen in lane 2, **1** was incorporated into the 3' end of **P1**, yielding a 19-nt product and a thin band (**) corresponding to the primer shortened by the 3' to 5' exonuclease activity. In other reactions with templates **T2**, **T3**, and **T4** containing G, C, and T, respectively (lanes 3–5), there was no 19-nt product, and denser bands were observed for the shortened primer. These results suggest that the dPz^O residue incorporated by Kf+ was resistant to 3' to 5' exonuclease activity. Thus, base pairing between Pz^O and A is recognized as legitimate by Kf+.

It was previously reported that 3-deaza-deoxyadenosine—which lacks a minor groove H-bond

acceptor—incorporated at the 3' end of a primer was excised by the exonuclease activity of Kf+.[28] This result indicated that Kf+ recognized the minor groove H-bond acceptor and distinguished between complementary and misincorporated nucleotides. The fact that dPz^O was not excised by Kf+ suggests that the N1 nitrogen of Pz^O acted as the minor groove H-bond acceptor, as in the case of the N3 of purine or 2-keto of pyrimidine nucleobases.

We carried out full-length chain elongation using primer **P1**, template **T1**, and the mixture of dATP, dGTP, and dCTP in the presence or absence of **1** or TTP and found that the full-length product was generated when **1** was used instead of TTP (Figure 10).

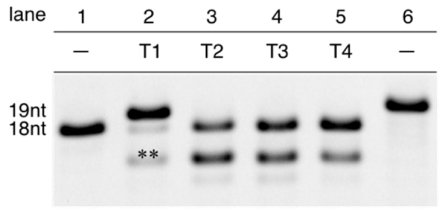

Figure 9. PAGE analysis of single nucleotide insertion using **1** to **P1** in the presence of 18-nt **T1**–**T4**. Lanes 1 and 6 correspond to synthetic 18-nt primer **P1** and 19-nt synthetic control **P2**, respectively. Conditions: 0.1 μM **T1**–**T4**; 0.1 μM **P1**; 10 μM each dNTP; 0.01 U/μl Kf−; reaction time = 10 min.

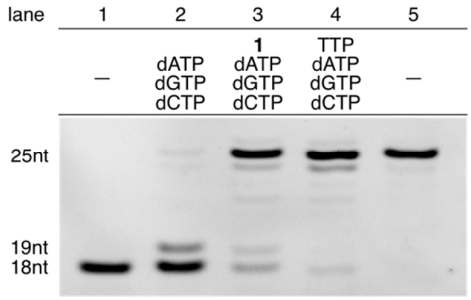

Figure 10. PAGE analysis of single nucleotide insertion using **1** to **P1** in the presence of 18-nt **T1**. Lanes 1 and 5 correspond to 18-nt primer **P1** and 25-nt synthetic control **P3**, respectively. Conditions: 0.1 μM **T1**; 0.1 μM **P1**; 10 μM each dNTP; 0.01 U/μl Kf−, and reaction time = 10 min.

Conclusion

In this study, we synthesized dPz^O (**13)** as well as its triphosphate **1** and phosphoramidite derivative **2**, and determined that Pz^O in DNA recognizes and selectively forms Watson-Crick base pairs with A. In addition, we demonstrated that **1** is incorporated into DNA by Kf− and Kf+, and was not excised by the 3' to 5' exonuclease activity. Finally, we found that **1** could be introduced at multiple sites as long as the template was designed so as to avoid consecutive A bases.

Compound **13** is a new thymidine analog lacking 2-keto and 5-methyl groups while maintaining Watson-Crick base-paring properties. Although similar pyrimidine deoxynucleoside analogs such as 5-(β-D-2-deoxyribofuranosyl)-3-methyl-2-pyridone and 5-(β-D-2-deoxyribofuranosyl)-2-aminopyridine—*C*-nucleosides with a methine instead of the 2-keto group—have been reported,[29] their properties as substrates of DNA polymerases are not known since they inhibit DNA polymerase reactions. We also demonstrated for the first time that the 2-keto group of pyrimidines is not essential for the DNA polymerase reaction, since **1**—which has a nitrogen atom that can form a hydrogen bond instead of the 2-keto group—was a substrate of Kf− and Kf+. Our results suggest that combining a base-pairing site with an endocyclic nitrogen atom *ortho* to the glycosidic bond is a promising design for novel artificial nucleoside triphosphates that can be incorporated into DNA by DNA polymerases. In the case of Pz^O, we combined a T-like hydrogen and endocyclic nitrogen atom, but other base pair motifs such as metal-mediated[30] or halogen bonding[31-33] interactions may be equally effective.

In its present form, compound **1** cannot be incorporated by Kf− in a consecutive manner. Although this property may be useful if **1** is used as a chain terminator at the consecutive position in antiviral or anticancer reagents,[34] it is nonetheless a limitation that must be overcome for broad application of this compound in synthetic biology. A possible reason for the failure of consecutive incorporation is the low stacking potential of Pz^O; the incorporation efficiency can in theory be improved by chemically modifying dPz^O so as to enhance the stacking interaction. Another reason is the lower hydrogen bonding capacity of the N1 of Pz^O with the amino acid residues of Kf+ and Kf−. As shown by the quantum chemical calculation of the G-Pz^O base pair, the hydrogen bonding capacity of the N1 of Pz^O was weaker than that of the 2-keto of T. Thus, DNA polymerases that can form strong hydrogen bonds with the N1 of Pz^O or that do not recognize the minor groove hydrogen bond acceptor with high stringency would be expected to efficiently incorporate **1**.

In this study, we used Kf− and Kf+ as DNA polymerases. These belong to family A, whose members directly recognize minor groove H-bond acceptors at the 3' end of primer and the counter nucleobase in the template via amino acid residues such as Arg and Gln.[35,36] On the other hand, RB69 polymerase—which belongs to family B—was found to recognize the N3 of A via Tyr567, which formed a water-mediated hydrogen bond.[37,12] This suggests that recognition of the minor groove H-bond site is more flexible in family B than in family A polymerases. Therefore, the potential for **1** to serve as a substrate for polymerases of family B as well as families C, D, X, and Y[38] merits further investigation.

We are currently developing new Pz^O derivatives and are screening polymerases to achieve more efficient incorporation of **1** and its derivatives. Moreover, a new artificial nucleobase bearing a nitrogen atom at the *ortho* position is being synthesized and will be reported elsewhere.

Experimental Section

General Methods

^{1}H, ^{13}C, ^{31}P- nuclear magnetic resonance (NMR) spectra were recorded at 500, 126, 202 MHz for ^{1}H, ^{13}C and ^{31}P-NMR, respectively. The chemical shifts were measured from the residual non-deuterated solvents of $CDCl_3$ (7.26 ppm), DMSO-*d* (2.49 ppm), CD_3OD-d_4 (3.31 ppm) and D_2O (4.79 ppm) for ^{1}H-NMR spectra, and solvents' signal of $CDCl_3$ (77.16 ppm), DMSO-d_6 (39.52 ppm) and CD_3OD-d_4 (49.00 ppm) for ^{13}C-NMR spectra and 85% phosphoric acid (0.00 ppm) for ^{31}P-NMR spectra. High-performance-liquid-chromatography (HPLC) analysis was run using reverse-phase (RP) C18 column (5 μm, 4.6 × 150 mm) or anion-exchange column (4 × 250 mm).

Measurements of UV-melting temperature

ODNs were dissolved in deionized distilled water and their concentration were determined from absorbance measurements at 260 nm. The absorption coefficients of ODNs were calculated according to the nearest–neighbor method[39] using the Oligo Analyzer 3.1 (http://sg.idtdna.com/calc/analyzer). The absorption coefficients of **ODN1** were calculated by assuming that they are identical to those of ODNs incorporating T instead of Pz^{O}.

The ODNs (1.2 nmol each) were dissolved in 10 mM sodium phosphate buffer (pH 7.0, 100 mM NaCl, 0.1 mM EDTA, 600 μL). The final concentration of the duplexes was 2 μM. The mixture was placed in quartz cells (10 mm) and incubated at 90 °C. After 10 min, the mixture was cooled to 5 °C then heated to 90 °C at a rate of 0.5 °C/min. The absorption at 260 nm was recorded and used to draw the UV-melting curves. The UV-melting curve was smoothed by the Savitzky–Golay method. Melting temperature was calculated as the temperature that gave the maximum of the first deviation of each UV melting curve.

Synthetic procedures

2-(2,3,5-Tri-*O*-acetyl-β-D-ribofuranosyl)furan (4)

1.0 M solution of $SnCl_4$ in CH_2Cl_2 (630 μL, 0.63 mmol) was added to a solution of tetra-*O*-acetyl-β-D-ribose (2.0 g, 6.28 mmol) and furan (960 μL, 12.6 mmol) in CH_2Cl_2 (32 mL) at 0 °C. The reaction mixture was stirred and warmed to ambient temperature for 2 h. The mixture was quenched with sat. $NaHCO_3$ aq. (300 mL). The mixture was filtered by celite® pad, and extracted twice with CH_2Cl_2 (100 mL each). The organic layers were combined and was dried over $MgSO_4$, filtered and evaporated under reduced pressure. The residue was purified by chromatography on a column of silica gel (60N, 50 g) using *n*-hexane–EtOAc (90:10–70:30, v/v) to give the fractions containing **4**. The fractions were collected and evaporated under reduced pressure to give **4** (625 mg, 31%).

^{1}H-NMR (500 MHz, DMSO-d_6): δ 2.01 (s, 3H, 2′-, 3′- or 5′-Ac), 2.03 (s, 3H, 2′-, 3′- or 5′-Ac),

2.07 (s, 3H, 2′-, 3′- or 5′-Ac), 4.08 (dd, 1H, *J* = 4.7 Hz, 12.0 Hz, H-5′), 4.21 (m, 1H, H-4′), 4.31 (dd, 1H, *J* = 3.4 Hz, 12.0 Hz, H-5′′), 4.95 (d, 1H, *J* = 6.5 Hz, H-1′), 5.25 (t, 1H, *J* = 5.2 Hz, H-3′), 5.35 (t, 1H, *J* = 6.1 Hz, H-2′), 6.46 (dd, 1H, *J* = 1.8 Hz, 3.2 Hz, aromatic-H), 6.54 (d, 1H, *J* = 3.2 Hz, aromatic-H), 7.71 (dd, 1H, *J* = 0.9 Hz, 1.8 Hz, aromatic-H); ^{13}C-NMR (126 MHz, DMSO-d_6): δ 20.3, 20.4, 20.6, 63.1, 71.2, 72.5, 74.8, 79.0, 109.9, 110.7, 143.9, 150.0, 169.4, 169.6, 170.0; ESI-TOF mass: calcd. for $C_{15}H_{18}NaO_8$ $[M+Na]^+$ 349.0894, found 349.0885.

2-(2,3,5-Tri-*O*-benzoyl-β-D-ribofuranosyl)furan (5)

Sodium methoxide (45 mg, 0.81 mmol) was added to a solution of **4** (2.56 g, 7.83 mmol) in MeOH (40 mL). The reaction mixture was stirred at ambient temperature for 1 h. The reaction mixture was evaporated under reduced pressure. The residue was dissolved in H_2O (40 mL), then the solution was passed through a DOWEX 50W X 8 (100–200 mesh, H^+ form, 14 mL). The fractions were collected and evaporated under reduced pressure to give a crude material. The residue was dissolved in pyridine (80 mL), and benzoyl chloride (3.7 mL, 31.3 mmol) was added. After 1 h, the reaction mixture was quenched with EtOH (5 mL). The reaction mixture was diluted with EtOAc (200 mL), washed twice with H_2O (150 mL each), twice with brine (150 mL each). The organic layer was dried over $MgSO_4$, filtered and evaporated under reduced pressure. The residue was purified by chromatography on a column of silica gel (C200, 100 g) using *n*-hexane–EtOAc (90:10–70:30, v/v) to give the fractions containing **5**. The fractions were collected and evaporated under reduced pressure to give **5** (3.75 g, 93%, 2 steps)

^{1}H-NMR (500 MHz, $CDCl_3$): δ 4.57–4.60 (dd, 1H, *J* = 4.2 Hz, 11.9 Hz, H-5′ or H-5′′), 4.69 (m, 1H, H-4′), 4.77 (dd, 1H, *J* = 3.4 Hz, 12.0 Hz, H-5′ or H-5′′), 5.32 (d, 1H, *J* = 4.9 Hz, H-1′), 5.90–5.95 (m, 1H, H-2′ and H-3′), 6.33–6.34 (m, 1H, aromatic-H), 6.45 (d, 1H, *J* = 3.0 Hz, aromatic-H), 7.34–7.44 (m, 8H, Bz-H), 7.52–7.57 (m, 4H, Bz-H and aromatic-H), 7.93–7.98 (m, 4H, Bz-H); ^{13}C-NMR (126 MHz, DMSO-d_6): δ 64.6, 72.9, 74.2, 75.8, 79.8, 110.7, 111.4, 129.2, 129.4, 129.5, 134.2, 134.5, 134.6, 144.6, 150.7, 165.2, 165.5, 166.1; ESI-TOF mass: calcd. for $C_{30}H_{24}NaO_8$ $[M+Na]^+$ 535.1363, found 535.1354.

4-(2,3,5-Tri-*O*-benzoyl-β-D-ribofuranosyl)-4-oxobutylic acid (7)

Concentrated sulfuric acid (6 mL) was added to a solution of chromium trioxide (5.0 g, 58.5 mmol) in water (18 mL). The mixture was stirred at 0 °C for 30 min. The 2.4 M Jones reagent (24 mL) was added to a solution of **5** (6.0 g, 11.7 mmol) in acetone (65 mL). The reaction mixture was stirred at 0 °C for 1 h. The reaction mixture was carefully poured into a two-layered mixture of CH_2Cl_2 (200 mL), and H_2O (200 mL) containing ice (50 g). The mixture was diluted with CH_2Cl_2 (100 mL), and extracted four times with CH_2Cl_2 (100 mL each). The organic layer was dried over $MgSO_4$, filtered and evaporated under reduced pressure. The residue was dissolved in EtOH (87 mL),

and to a suspention of 5% palladium-carbon (470 mg) in EtOH (7 mL) was added. The reaction mixture was stirred at ambient temperature for 1 h. The mixture was filtered on celite® pad, and the solvent was evaporated under reduced pressure. The residue was purified by chromatography on a column of silica gel (C300, 80 g) using *n*-hexane–EtOAc (50:50–10:90, v/v) to give the fractions containing **7**. The fractions were collected and evaporated under reduced pressure to give **7** (4.42 g, 93%, 2 steps).

^{1}H-NMR (500 MHz, DMSO-d_6): δ 2.46 (m, 2H, -C(O)CH$_2$*CH$_2$*-), 2.81–2.98 (m, 2H, -C(O)*CH$_2$*CH$_2$-), 4.58–4.61 (m, 1H, H-5′ or H-5′′), 4.65–4.68 (m, 1H, H-5′ or H-5′′), 4.73 (m, 1H, H-4′), 4.92 (m, 1H, H-1′), 5.66 (t, 1H, *J* = 5.9 Hz, H-3′), 5.89 (t, 1H, *J* = 4.9 Hz, H-2′), 7.39 (t, 2H, *J* = 7.7 Hz, Bz-H), 7.47 (t, 4H, *J* = 7.7 Hz, Bz-H) 7.58–7.66 (m, 3H, Bz-H), 7.82–7.99 (m, 6H, Bz-H), 12.4 (br, 1H, -C(O)*OH*); ^{13}C-NMR (126 MHz, DMSO-d_6): δ 28.0, 34.1, 64.6, 72.5, 73.6, 79.7, 85.5, 129.2, 129.3, 129.4, 129.5, 129.8, 129.9, 130.0, 134.2, 134.4, 134.5, 165.2, 165.3, 166.2, 174.4, 207.2; ESI-TOF mass: calcd. for $C_{30}H_{26}NaO_{10}$ $[M+Na]^+$ 569.1418, found 569.1414.

6-(2,3,5-Tri-*O*-benzoyl-β-D-ribofuranosyl)-4,5-dihydropyridazin-3-one (8)

Hydrazine monohydrate (140 μL, 4.25 mmol) and 4-(4,6-dimethoxy-1,3,5-triazin-2-yl)-4-methylmorpholinium chloride (1.18 g, 4.25 mmol) was added to a solution of **7** (1.53 g, 2.83 mmol) in dry EtOH (84 mL). The reaction mixture was stirred at ambient temperature for 2 h. The mixture was diluted with *n*-hexane–EtOAc (200 mL, 1:1, v/v), washed twice with H_2O (150 mL each), and twice with brine (150 mL each). The organic layer was dried over $MgSO_4$, filtered and evaporated under reduced pressure. The residue was purified by chromatography on a column of silica gel (60N, 100 g) using *n*-hexane–EtOAc (70:30–50:50, v/v) to give the fractions containing **8**. The fractions were collected and evaporated under reduced pressure to give **8** (1.07 g, 70%).

^{1}H-NMR (500 MHz, $CDCl_3$): δ 2.38–2.48 (m, 2H, H-5), 2.57–2.69 (m, 2H, H-4), 4.53 (dd, 1H, *J* = 3.6 Hz, 12.2 Hz, H-5′ or H-5′′), 4.66–4.68 (m, 1H, H-4′), 4.80–4.83 (m, 2H, H-1′ and H-5′ or H-5′′), 5.82 (t, 1H, *J* = 4.4 Hz, H-3′), 5.85 (t, 1H, *J* = 6.0 Hz, H-2′), 7.35–7.49 (m, 6H, Bz-H), 7.53–7.61 (m, 3H, Bz-H), 7.93–8.09 (m, 6H, Bz-H), 8.27 (br, 1H, N-H); ^{13}C-NMR (126 MHz, $CDCl_3$): δ 21.1, 26.1, 64.0, 72.7, 72.9, 80.9, 82.4, 128.7, 128.8, 128.9, 129.0, 129.2, 129.6, 129.6, 130.0, 133.7, 133.8, 133.9, 151.2, 165.6, 165.7, 166.3, 167.4; ESI-TOF mass: calcd. for $C_{30}H_{26}N_2NaO_8$ $[M+Na]^+$ 565.1581, found 565.1566.

6-(2,3,5-Tri-*O*-benzoyl-β-D-ribofuranosyl)pyridazin-3-one (9)

2,3-dichloro-5,6-dicyanobenzoquinone (840 mg, 3.68 mmol) and *p*-toluenesulfonic acid monohydrate (350 mg, 1.84 mmol) was added to a solution of **8** (1.0 g, 1.84 mmol) in dry toluene (45 mL). The reaction mixture was stirred at ambient temperature for 2 h. The reaction mixture was

diluted with EtOAc (300 mL), washed twice with sat. $NaHCO_3$ aq. (300 mL, each), once brine (300 mL). The organic layer was dried over $MgSO_4$, filtered and evaporated under reduced pressure. The residue was purified by chromatography on a column of silica gel (N-H, 20 g) using *n*-hexane–EtOAc (70:30–30:70, v/v) to give the fractions containing **9**. The fractions were collected and evaporated under reduced pressure to give **9** (680 mg, 68%).

^{1}H-NMR (500 MHz, DMSO-d_6): δ 4.59 (dd, 1H, J = 4.5 Hz, 12.1 Hz, H-5′ or H-5′′), 4.65 (1H, dd, J = 3.6 Hz, 12.2 Hz, H-5′ or H-5′′), 4.74–4.77 (m, 1H, H-4′), 5.19 (d, 1H, J = 5.9 Hz, H-1′), 5.79 (t, 1H, J = 5.4 Hz, H-3′), 5.91 (t, 1H, J = 5.8 Hz, H-2′), 6.89 (d, 1H, J = 9.8 Hz, H-4), 7.42–7.52 (m, 6H, Bz-H), 7.57 (d, 1H, J = 9.8 Hz, H-5), 7.62–7.68 (m, 3H, Bz-H), 7.85–7.93 (m, 6H, Bz-H), 13.1 (br, 1H, N-H); ^{13}C-NMR (126 MHz, DMSO-d_6): δ 64.0, 72.3, 73.9, 79.9, 80.6, 128.7, 128.8, 129.0, 129.1, 129.1, 129.4, 129.5, 129.5, 130.7, 132.3, 133.9, 134.1, 134.2, 144.3, 160.8, 164.9, 165.0, 165.8; ESI-TOF mass: calcd. for $C_{30}H_{24}N_2O_8Na$ $[M+Na]^+$ 563.1425, found 563.1418.

6-(β-D-ribofuranosyl)pyridazin-3-one (10)

28% NH_3 aq. (19 mL) was added to a solution of **9** (1.3 g, 2.41 mmol) in MeOH (12 mL). The reaction mixture was sealed and heated at 80 °C for 12 h. After being cooled to the ambient temperature, the solvent was evaporated under reduced pressure. The residue was purified by chromatography on a column of silica gel (C200, 10 g) using CH_2Cl_2–MeOH (100:0–80:20, v/v) to give the fractions containing **10**. The fractions were collected and evaporated under reduced pressure to give **10** (468 mg, 85%).

^{1}H-NMR (500 MHz, CD_3OD-d_4): δ 3.65–3.68 (dd, 1H, J = 4.2 Hz, 12.1 Hz, H-5′ or H-5′′), 3.73–3.77 (dd, 1H, J = 3.4 Hz, 12.1 Hz, H-5′ or H-5′′), 3.97–3.99 (m, 1H, H-4′), 4.07–4.12 (m, 2H, H-2′ and H-3′), 4.63 (d, 1H, J = 6.5 Hz, H-1′), 6.97 (d, 1H, J = 9.8 Hz, H-4), 7.71 (d, 1H, J = 9.8 Hz, H-5); ^{13}C-NMR (126 MHz, CD_3OD-d_4): δ 63.3, 73.0, 76.9, 83.9, 87.0, 130.8, 133.9, 149.4, 163.8; ESI-TOF mass: calcd. for $C_9H_{11}N_2O_5$ $[M–H]^-$ 227.0673, found 227.0668.

UV-vis spectrum (in 10 mM sodium phosphate buffer pH 7.0), λ_{max} = 284 nm (ε = 2.43 × 10^3)

6-[3,5-*O*-(1,1,3,3-Tetraisopropyldisiloxane-1,3-diyl)- β-D-ribofuranosyl]pyridazin-3-one (11)

Compound **10** (350 mg, 1.43 mmol) was co-evaporated four times with pyridine, and dissolved in dry pyridine (15 mL) under an argon atmosphere. To the solution of **10** were added 1,3-dichloro-1,1,3,3-tetraisopropyldisiloxane (540 μL, 1.68 mmol). The mixture was stirred at ambient temperature for 15 h. The reaction mixture was quenched with EtOH (5 mL). The reaction mixture was diluted with EtOAc (100 mL) washed twice with H_2O (100 mL), and twice with brine (100 mL each). The organic layer was dried over $MgSO_4$, filtered and evaporated under reduced pressure. The residue was purified by chromatography on a column of silica gel (60N, 20 g) using *n*-hexane–EtOAc (90:10–30:70, v/v) to give the fractions containing **11**. The fractions were collected and

evaporated under reduced pressure to give **11** (504 mg, 70%).

^{1}H-NMR (500 MHz, DMSO-d_6): δ 0.97–1.03 (m, 28H, TIPDS-H), 3.85–3.90 (m, 2H, H-4, and H-5′ or 5′′), 3.99 (dd, 1H, J = 3.2 Hz, 12.4 Hz, H-5′ or 5′′), 4.09 (dd, 1H, J = 5.1 Hz, 8.0 Hz, H-3′), 4.14–4.16 (m, 1H, H-2′), 4.56 (d, 1H, J = 1.7 Hz, H-1′), 5.28 (d, 1H, J = 5.0 Hz, 2′-OH), 6.85 (d, 1H, J = 9.8 Hz, H-4), 7.44 (d, 1H, J = 9.8 Hz, H-5), 12.9 (s, 1H, N-H); ^{13}C-NMR (126 MHz, DMSO-d_6): δ 12.0, 12.2, 12.5, 12.8, 16.8, 16.9, 17.0, 17.1, 17.2, 17.4, 60.9, 70.8, 74.2, 81.1, 83.8, 130.0, 131.4, 146.1, 160.4; ESI-TOF mass: calcd. for $C_{21}H_{37}N_2O_6Si_2$ $[M–H]^-$ 469.2196, found 469.2195.

6-[3,5-*O*-(1,1,3,3-Tetraisopropyldisiloxane-1,3-diyl)-2-deoxy-β-D-ribofuranosyl]pyridazin-3-one (12)

N,*N*-dimethyl-4-aminopyridine (640 mg, 5.1 mmol) and *O*-phenylchlorothionoformate (350 μL, 2.55 mmol) was added to a solution of **11** (800 mg, 1.70 mmol) in dry MeCN (34 mL). The reaction mixture was stirred at ambient temperature for 1 h. The reaction mixture was evaporated under reduced pressure to give a crude material. This material was dissolved in dry toluene (36 mL), and 2,2′-azodiisobutyronitrile (26 mg, 0.14 mmol), tris(trimethylsilyl)silane (665 μL, 2.16 mmol) were added. The reaction mixture was stirred at 90 °C for 15 h. The reaction mixture was diluted with EtOAc (100 mL), and washed twice with 5% NaClO aq. (150 mL each). The organic layer was dried over $MgSO_4$, filtered and evaporated under reduced pressure. The residue was purified by chromatography on a column of silica gel (60N, 15 g) using *n*-hexane–EtOAc (80:20–50:50, v/v) to give the fractions containing **12**. The fractions were collected and evaporated under reduced pressure to give **12** (498 mg, 76%).

^{1}H-NMR (500 MHz, $CDCl_3$): δ 1.01–1.08 (m, 28H, TIPDS-H), 2.26–2.32 (m, 1H, H-2′ or 2′′), 2.34–2.39 (m, 1H, H-2′ or 2′′), 3.82–3.87 (m, 2H, H-5′ and 5′′), 4.03–4.07 (m, 1H, H-4′), 4.44–4.78 (m, 1H, H-3′), 4.98 (dd, 1H, J = 6.5 Hz, 7.5 Hz, H-1′), 6.80 (d, 1H, J = 9.8 Hz, H-4), 7.47 (d, 1H, J = 9.8 Hz, H-5), 11.8 (s, 1H, N-H); ^{13}C-NMR (126 MHz, $CDCl_3$): δ 12.7, 13.1, 13.4, 13.6, 17.1, 17.2, 17.2, 17.4, 17.5, 17.5, 17.5, 17.7, 39.6, 62.8, 72.1, 86.2, 130.6, 132.0, 148.9, 162.0.; ESI-TOF mass: calcd. for $C_{21}H_{38}N_2NaO_5Si_2$ $[M+Na]^+$ 477.2211, found 477.2204.

6-(2-Deoxy-β-D-ribofuranosyl)pyridazin-3-one (13)

Triethylamine (455 μL, 3.24 mmol) and triethylamine trihydrofluoride (530 μL, 3.24 mmol) were added to a solution of **12** (490 mg, 1.08 mmol) in dry THF (11 mL). The reaction mixture was stirred at ambient temperature for 16 h. The reaction was quenched with trimethylethoxysilane (840 μL, 5.40 mmol). The mixture was evaporated under reduced pressure. The residue was purified by chromatography on a column of silica gel (60N, 5 g) using CH_2Cl_2–MeOH (100:0–80:20, v/v) to give the fractions containing **13**. The fractions were collected and evaporated under reduced pressure to give **13** (170 mg, 73%).

^{1}H-NMR (500 MHz, CD_3OD-d_4): δ 2.11–2.15 (m, 2H, H-2′ and H-2′′), 3.01–3.67 (m, 2H, H-5′ and H-5′′), 3.94 (m, 1H, H-4′), 4.34 (m, 1H, H-3′), 5.01 (dd, 1H, J = 7.1 Hz, 9.3 Hz, H-1′), 6.97 (d, 1H, J = 9.8 Hz, H-4), 7.71 (d, 1H, J = 9.8 Hz, H-5); ^{13}C-NMR (126 MHz, CD_3OD-d_4): δ 42.0, 63.7, 74.1, 79.8, 89.6, 130.9, 133.9, 150.5, 163.8; ESI-TOF mass: calcd. for $C_9H_{12}N_2NaO_4$ $[M+Na]^+$ 235.0689, found 235.0691.

1*R*-1,2-dideoxy-1-(3-oxo-2*H*-pyridazin-6-yl)ribofuranose 5-triphosphate tris(triethylammonium) salt (1)

To a solution of **12** (21 mg, 0.1 mmol) in trimethyl phosphate (500 μL), phosphoryl chloride (12 μL, 0.13 mmol) was added at 0 °C. The reaction mixture was stirred at 0 °C for 1 h. Tri-*n*-butylamine (100 μL, 0.42 mmol) was added to the reaction mixture, and then 0.5 M bis(tributylammonium) pyrophosphate in a DMF solution (500 μL) was added. After 2 h, the reaction was quenched by the addition of 2.0 M triethylammonium bicarbonate (TEAB, 1.0 mL). The resulting crude product was purified by 1.5 cm × 20 cm DEAE Sephadex A-25 column chromatography (eluted by a linear gradient of 50 mM TEAB to 1.0 M TEAB), and then by RP-HPLC (eluted by a linear gradient of MeCN, 0% to 15% in 0.1 M triethylammonium acetate buffer) to give **1** (26.8 μmol, 27%).

^{1}H-NMR (500 MHz, D_2O): δ 2.26 (m, 2H, H-2′ and H-2′′), 4.09 (m, 2H, H-5′ and H-5′′), 4.23 (m, 1H, H-4′), 4.60 (m, 1H, H-3′), 5.11 (t, 1H, J = 8.3 Hz, H-1′), 7.15 (d, 1H, J = 9.8 Hz, H-4), 7.83 (d, 1H, J = 9.8 Hz, H-5); ^{31}P-NMR (202 MHz, D_2O): δ –22.99 (t, J = 19.8 Hz), –11.09 (d, J = 19.9 Hz), –10.49 (d, J = 19.4 Hz); ESI-TOF mass: calcd. for $C_9H_{14}N_2O_{13}P_3$ $[M–H]^–$ 450.9714, found 450.9714.

6-(5′-*O*-Dimethoxytrityl-2-deoxy-β-D-ribofuranosyl)pyridazin-3-one (14)

Compound **13** (85 mg, 0.4 mmol) was co-evaporated four times with pyridine, and dissolved in dry pyridine (4 mL) in under an argon atmosphere. To the solution of **13** was added 4,4′-dimethoxytrityl chloride (169 mg, 0.48 mmol). The mixture was stirred at ambient temperature for 4 h. The reaction was quenched with EtOH (1 mL). The reaction mixture was diluted with CH_2Cl_2 (15 mL) washed twice with H_2O (15 mL each), and twice with brine (15 mL each). The organic layer was dried over $MgSO_4$, filtered and evaporated under reduced pressure. The residue was purified by chromatography on a column of silica gel (60N, 6 g) using CH_2Cl_2–MeOH (100:0–90:10, v/v) to give the fractions containing **14**. The fractions were collected and evaporated under reduced pressure to give **14** (110 mg, 53%).

^{1}H-NMR (500 MHz, DMSO-d_6): δ 2.00–2.13 (m, 2H, H-2′ and H-2′′), 3.01 (dd, 1H, J = 5.3 Hz, 10.1 Hz, H-5′ or H-5′′), 3.07 (dd, 1H, J =3.8 Hz, 10.1 Hz, H-5′ or H-5′′), 3.72 (s, 6H, DMTr-OCH_3), 3.89–3.91 (m, 1H, H-4′), 4.16–4.17 (m, 1H, H-3′), 4.90 (dd, 1H, J = 6.1 Hz, 9.4 Hz,

H-1′), 5.18 (br, 1H, H-4), 6.85–6.87 (m, 5H, DMTr-H), 7.19–7.23 (m, 5H, DMTr-H), 7.27–7.30 (m, 2H, DMTr-H), 7.34–7.36 (m, 2H, DMTr-H), 7.41–7.43 (m, 1H, H-5), 12.9 (br, 1H, N-H); ^{13}C-NMR (126 MHz, DMSO-d_6): δ 55.0, 55.1, 64.2, 72.2,77.9, 78.0, 85.4, 86.3, 113.2, 126.7, 127.7, 127.8, 129.70, 129.73, 130.2, 131.8, 135.6, 144.9, 147.2, 158.0, 160.6; ESI-TOF mass: calcd. for $C_{30}H_{30}N_2NaO_6^+$ $[M+Na]^+$ 537.1996, found 537.2001.

1*R*-1,2-dideoxy-5-*O*-(4,4′-dimethoxytrityl)-1-(3-oxo-2*H*-pyridazin-6-yl)ribofuranose 3-(2-cyanoethyl *N, N*-diisopropylphosphoramidite) (2)

Compound **14** (100 mg, 0.19 mmol) was co-evaporated four times each with pyridine and toluene, and dissolved in dry CH_2Cl_2 (2 mL) in under an argon atmosphere. *N, N*-diisopropylethylamine (86 μL, 0.49 mmol) and 2-cyanoethyl *N, N*-diisopropylchlorophosphoramidite (55 μL, 0.25 mmol) was added to a solution of **14**. The mixture was stirred at ambient temperature for 30 min. The reaction mixture was diluted with CH_2Cl_2 (10 mL), washed three times with $NaHCO_3$ aq. (15 mL each), and twice with brine (15 mL each). The organic layer was dried over $MgSO_4$, filtered and evaporated under reduced pressure. The residue was purified by chromatography on a column of silica gel (60N, 3 g) using CH_2Cl_2–MeOH (100:0–95:5, v/v) to give the fractions containing **2**. The fractions were collected and evaporated under reduced pressure to give **2** (68 mg, 50%).

^{1}H-NMR (500 MHz, $CDCl_3$): δ 1.09–1.19 (m, 12H, -CH(CH_3)$_2$), 2.16–2.42 (m, 2H, H-2′ and H-2′′), 2.45 (t, 1H, J = 6.5 Hz), 2.61 (t, 1H, J = 6.4 Hz), 3.20–3.32 (m, 1H, H-5′ and H-5′′), 3.54–3.62 (m, 2H, -CH(CH_3)$_2$-), 3.54–3.85 (m, 10H, -$CH_2$$CH_2$CN, -$CH_2$$CH_2$CN, DMTr-O$CH_3$), 4.21–4.24 (m, 1H, H-4′), 4.53–4.56 (m, 1H, H-3′), 5.02–5.25 (m, 1H, H-1′), 6.80–6.86 (m, 5H, DMTr-H), 7.19–7.25 (m, 5H, DMTr-H and H-4), 7.27–7.31 (m, 2H, DMTr-H), 7.40–7.42 (m, 2H, DMTr-H), 7.41–7.43 (m, 1H, H-5), 10.7 (br, 1H, N-H); ^{13}C-NMR (126 MHz, $CDCl_3$): δ 20.., 20.38, 20.39, 20.52, 20.58, 24.60, 24.67, 24.71, 24.73, 24.77, 24.79, 39.35, 40.26, 40.29, 40.38, 40.40, 43.27, 43.34, 43.38, 43.44, 55.36, 55.37, 55.39, 55.41, 58.25, 58.29, 58.30, 58.40, 58.43, 58.44, 63.91, 64.02, 75.40, 75.53, 75.72, 75.85, 78.61, 78.66, 86.24, 86.26, 86.59, 86.30, 86.44, 86.45, 86.51, 86.54, 113.25, 117.58, 117.67, 127.03, 127.04, 127.97, 128.28, 128.33, 130.20, 130.24, 130.73, 132.20, 135.87, 135.90, 144.74, 144.77, 148.48, 148.51, 158.65, 158.66, 161.16; ^{31}P-NMR (202 MHz, $CDCl_3$): δ 149.2, 149.5; ESI-TOF mass: calcd. for $C_{39}H_{47}N_4NaO_7P^+$ $[M+Na]^+$ 737.3075, found 737.3065.

Single-nucleotide insertion by Kf– or Kf+

The equimolar amount of the template DNA and **P1** were mixt in a 5 μL of buffer containing 100 mM NaCl, 20 mM Tris-HCl (pH 7.9), 20 mM $MgCl_2$ and 2 mM DTT so that the final concentration of the duplex became 0.2 μM. The duplex was annealed by heating at 90 °C for 1 min and slow

cooling to ambient temperature. The duplex mixture (5 μL) was mixed with a solution containing Kf– (0.1 Unit·μL^{-1}, 1 μL). Then, the mixture was incubated at 37 °C for 2 min. The reactions were initiated by adding a solution containing **1** (25 μM, 4 μL) to the DNA–enzyme mixture at 37 °C. The reaction mixture was incubated for 10 min at 37 °C and quenched by the addition of 20 μL of stop solution (10 M Urea, 50 mM EDTA, 0.1% BPB solution). After vigorous stirring, the 3 μL aliquot of reaction mixtures were analyzed by electrophoresis with 20% denaturing polyacrylamide gel containing 7 M urea (40 W, 55 °C, 60 min) and visualized in fluoroimage analyzer (FUJIFILM FLA–9500).

Steady-state kinetics of single-nucleotide insertion by Kf–

Equal amount of **T1** and **P1** were dissolved in 3 μL of buffer containing 500 mM NaCl, 100 mM Tris–HCl, 100 mM $MgCl_2$ and 10 mM DTT so that the final concentration of the duplex to 0.5–2.5 μM. Then **T1** was annealed with **P1** by heating at 90 °C for 1 min and following slow cooling to ambient temperature. The duplex mixture (3 μL) was mixed with a solution containing Kf–(0.025–2.5 Unit·μL^{-1}, 2 μL). Then, the mixture was incubated at 37 °C for 2 min. The reactions were initiated by adding a solution containing **1** (2–10 μM, 5 μL) or TTP (0.04–240 μM, 5 μL) to the at 37 °C. The reaction mixture was incubated for 1 min at 37 °C and quenched by the addition of 20 μL of stop solution (10 M urea, 50 mM EDTA, 0.1% BPB solution). After vigorous stirring, 3 μL aliquots of the reaction mixtures were analyzed by electrophoresis with 20% denaturing polyacrylamide gel containing 7 M urea (40 W, 55 °C, 60 min) and visualized on fluoroimage analyzer (FUJIFILM FLA–9500). The kinetic parameters (K_m and V_{max}) were determined from Hanes–Woolf plots.

Chain elongation reaction using Kf– or Kf+ in the presence of various dNTPs

The equimolar amount of the template DNA and **P1** were mixed in a 5 μL of buffer containing 100 mM NaCl, 20 mM Tris-HCl (pH 7.9), 20 mM $MgCl_2$ and 2 mM DTT so that the final concentration of the duplex became 0.2 μM. The duplex was annealed by heating at 90 °C for 1 min and slow cooling to ambient temperature.

The duplex mixture (5 μL) was mixed with a solution containing Kf– (0.1 Unit·μL^{-1}, 1 μL). Then, the mixture was incubated at 37 °C for 2 min. The reactions were initiated by adding a 4 μL of the solution containing **1** (25 μM), dATP (25 μM), dGTP (25 μM) and dCTP (25 μM) to the DNA–enzyme mixture at 37 °C. The reaction mixture was incubated for 10 min at 37 °C and quenched by the addition of 20 μL of stop solution (10 M Urea, 50 mM EDTA, 0.1% BPB solution). After vigorous stirring, the 3 μL aliquot of the reaction mixtures were analyzed by electrophoresis with 20% denaturing polyacrylamide gel containing 7 M urea (40 W, 55 °C, 60 min) and visualized in fluoroimage analyzer (FUJIFILM FLA–9500).

Supporting Information

The Supporting Information is available free of charge on the ACS Publications website. General procedure, HPLC charts, MALDI-TOF mass charts, UV-melting curves, and HPLC charts, Coordinates used for the quantum chemical calculations, and the calculated energies and frequencies are included.

Acknowledgement

This study was financially supported by JSPS KAKENHI 17H05230, 26288075, 17H04886.

References

1) Sismour, A. M.; Benner, S. A. The Use of Thymine Analogs to Improve the Replication of an Extra DNA Base Pair: A Synthetic Biological System. *Nucleic Acids Res.* **2005**, *33*, 5640-5646.

2) Benner, S. A. Understanding Nucleic Acids Using Synthetic Chemistry. *Acc. Chem. Res.* **2004**, *37*, 784-797.

3) Benner, S. A. Redesigning Genetics. *Science* **2004**, *306*, 625-626.

4) Zhang, Y.; Lamb, B. M.; Feldman, A. W.; Zhou, A. X.; Lavergne, T.; Li, L.; Romesberg, F. E. A Semisynthetic Organism Engineered for the Stable Expansion of the Genetic Alphabet. *Proc. Natl. Acad. Sci. USA* **2017**, *114*, 1317–1322.

5) Malyshev, D. A.; Dhami, K.; Quach, H. T.; Lavergne, T.; Ordoukhanian, P.; Torkamani, A.; Romesberg, F. E. Efficient and Sequence-Independent Replication of DNA Containing a Third Base Pair Established Functional Six-Letter Genetic Alphabet. *Proc. Natl. Acad. Sci. USA* **2012**, *109*, 12005–12010.

6) Hirao, I.; Mitsui, T.; Kimoto, M.; Yokoyama, S. An Efficient Unnatural Base Pair for PCR Amplification. *J. Am. Chem. Soc.* **2007**, *129*, 15549–15555.

7) Kimoto, M.; Yamashige, R.; Matsunaga, K. –I.; Yokoyama, S.; Hirao, I. Generation of High-Affinitiy DNA Aptamers Using an Expanded Genetic Alphabet. *Nature Biotech.* **2013**, *31*, 453–457.

8) Yang, Z.; Sismour, A. M.; Sheng, P.; Puskar, N. L.; Benner, S. A. Enzymatic Incorporation of Third nucleobase pair. *Nucleic Acids Res.* **2007**, *35*, 4238–4249.

9) Moran, S.; Ren, R. X. –F.; Kool, E. T. A thymidine triphosphate shape analog locking Watson-Crick Pairing Ability Is Replicated with High Sequence Selectivity. *Proc. Natl. Acad. Sci. USA* **1997**, *94*, 10506–10511.

10) Betz, K.; Malyshev, D. A.; Lavergne, T.; Welte, W.; Diederichs, K.; Dwyer, T. J.; Ordoukhanian, P.; Romesberg, F. E.; Marx, A. KlenTaq Polymerase Replicate Unnatural Base Pairs by Inducing a Watson–Crick Geometry. *Nature Chem. Biol.* **2012**, *8*, 612–614.

11) Li, Y.; Waksman, G. Crystal Structures of a ddATP-, ddTTP-, ddCTP-, and ddGTP-Trapped Ternary Complex of Klentaq1: Insights into Nucleotide Incorporation and Selectivity. *Prot. Sci.* **2001**, *10*, 1225–1233.

12) Xia, S.; Konigsberg, W. H. RB69 DNA Polymerase Structure, Kinetics, and Fidelity. *Biochemistry* **2014**, *53*, 2752–2767.

13) Betz, K.; Kimoto, M.; Diederichs, K.; Hirao, I.; Marx, A. Structural Basis for Expansion of the Genetic Alphabet with an Artificial Nucleobase Pair. *Angew. Chem. Int. Ed.* **2017**, *56*, 12000–12003.

14) Matsuda, S.; Henry, A. A.; Schultz, P. G.; Romesberg, F. E. The Effect of Minor-Groove Hydrogen-Bond Acceptors and Donors on the Stability and Replication of Four Unnatural Base Pairs. *J. Am. Chem. Soc.* **2003**, *125*, 6134–6139.

15) Kim, Y.; Leconte, A. M.; Hari, Y.; Romesberg, F. E. Stability and Polymerase Recognition of Pyridine Nucleobase Analogues: Role of Minor-Groove H-Bond Acceptors. *Angew. Chem. Int. Ed.* **2006**, *45*, 7809–7812.

16) Zhao, Y.; Truhlar, D. G. The M06 Suite of Density Functionals for Main Group Thermochemistry, Thermochemical Kinetics, Noncovalent Interactions, Excited States, and Transition Elements: Two New Functionals and Systematic Testing of Four M06-Class Functionals and 12 Other Functionals. *Theor. Chem. Acc.* **2008**, *120*, 215–241.

17) Boys, S. F.; Bernardi, F. The Calculation of Small Molecular Interactions by the Differences of Separate Total Energies. Some procedures with Reduced Errors. *Mol. Phys.* **1970**, *19*, 553–556.

18) Sun, Z.; Ahmed, S.; McLaughlin, L. W. Syntheses of Pyridin C-Nucleoside as Analogues of the Natural Nucleoside dC and dU. *J. Org. Chem.* **2006**, *71*, 2922-2925.

19) Joubert, N.; Pohl, R.; Klepetářová, B.; Hocek, M. Modular and Practical Synthesis of 6-Substituted Pyridin-3-yl C-Nucleosides. *J. Org. Chem.* **2007**, *72*, 6797-6805.

20) Maeba, I.; Iwata, K; Usami, F.; Furukawa, H. *C*-Nucleosides. 1. Synthesis of 3-(β-D-Ribofuranosyl)pyridazines. *J. Org. Chem.* **1983**, *48*, 2998–3002.

21) Maeba, I.; Suzuki, M.; Hara, O.; Takeuchi, T.; Iijima, T.; Furukawa, H. *C*-Nucleosides. 6. Synthesis of 5-Methoxy-5-(2,3,5-tri-*O*-benzoyl-β-D-ribofuranosyl)furan-2(5H)-one and Its Ring Transformation. *J. Org. Chem.* **1987**, *52*, 4521–4526.

22) Maeba, I.; Iijima, T.; Matsuda, Y.; Ito, C. *C*-Nucleoside. 12.† Synthesis of 2′-Deoxy Pyridazinone *C*-nucleoside from 2-(2.3.5-Tri-*O*-benzoyl-β-D-ribofuranosyl)furan. *J. Chem. Soc. Perkin Trans. 1* **1990**, 73–76.

23) Spadafora, M.; Mehiri, M.; Burger, A.; Benhida, R. Friedel–Crafts and Modified Vorbrüggen Ribosylation. A Short Synthesis of Aryl and Heteroaryl-*C*-nucleosides. *Tetrahedron Lett.* **2008**, *49*, 3967–3971.

24) Yoshikawa, M.; Kato, T.; Takenishi, T. A Novel Method for Phosphorylation of Nucleoside to 5′-Nucleotides. *Tetrahedron Lett.* **1967**, *50*, 5065–5068.

25) Yoshikawa, M.; Kato, T.; Takenishi, T. Studies of Phosphorylation. III. Selective Phospholylation of Unprotected Nucleosides. *Bull. Chem. Soc. Japan* **1969**, *42*, 3505–3508.

26) Clark, J. M.; Joyce, C. M.; Beardsley, G. P. Novel Blunt-end Addition Reactions Catalyzed by DNA Polymerase I of *Escherichia coli*. *J. Mol. Biol.* **1987**, *198*, 123–127.

27) Xia, S.; Vashishtha, A.; Bulkley, D.; Eom, S. H.; Wang, J.; Konigsberg, W. H. Contribution of Partial Charge Interactions and Base-Stacking to the Efficiency of Primer-Extension at and beyond Abasic Sites in DNA. *Biochemistry* **2012**, *51*, 4922–4931.

28) Hendrickson, C. L.; Devine, K. G. Benner, S. A. Probing Minor Groove Recognition Contacts by DNA Polymerases and Reverse Transcriptases Using 3-Deaza-2′-deoxyadenosine. *Nucleic Acids Res.* **2004**, *32*, 2241–2250.

29) Guo, M.-J.; Hildbrand, S.; Leumann, C. J.; McLaughlin, L. W.; Waring, M. J. Inhibition of DNA Polymerase Reactions by Pyrimidine Nucleotide Analogues Lacking the 2-Keto Group. *Nucleic Acids Res.* **1998**, *26*, 1863–1869.

30) Kobayashi, T.; Takezawa, Y.; Sakamoto, A.; Shionoya, M. Enzymatic Synthesis of Ligand-Bearing DNAs for Metal-Mediated Base Pairing Utilizing a Template-Independent Polymerase. *Chem. Commun.* **2016**, *52*, 3762–3765.

31) Solomon, R. V.; Vedha, S. A.; Venuvanalingam, P. A New Turn in Codon–Anticodon Selection Through Halogen Bonds. *Phys. Chem. Chem. Phys.* **2014**, *16*, 7430–7440.

32) Parker, A. J.; Stewart, J.; Donald, K. J.; Parish, C. A. Halogen Bonding in DNA Base Pairs. *J. Am. Chem. Soc.* **2012**, *134*, 5165–5172.

33) Tawarada, R.; Seio, K.; Sekine, M. Synthesis and Properties of Oligonucleotides with Iodo-Substitutes Aromatic Aglycons: Investigation of Possible Halogen Bonding Base Pairs. *J. Org. Chem.* **2008**, *73*, 383–390.

34) Berdis, A. J. DNA Polymerases as Therapeutic Targets. *Biochemistry* **2008**, *47*, 8253–8260.

35) Singh, K.; Modak, M. J. Presence of 18-Å Long Hydrogen Bond Track in the Active Site of *Escherichia coli* DNA Polymerase I (Klenow fragment). *J. Biol. Chem.* **2003**, *278*, 11289–11302.

36) Spratt, T. E. Identification of Hydrogen Bonds between *Escherichia coli* DNA Polymerase I (Klenow fragment) and the Minor Groove of DNA by Amino Acid Substitution of the Polymerase and Atomic Substitution of the DNA. *Biochemistry* **2001**, *40*, 2647–2652.

37) Xia, S.; Christian, T. D.; Wang, J.; Konigsberg, W. H. Probing Minor Groove Hydrogen Bonding Interactions between RB69 DNA Polymease and DNA. *Biochemistry*, **2012**, *51*, 4343–4353.

38) Filée, J.; Forterre, P.; Sen-Lin, T.; Laurent, J. *J. Mol. Evol.* Evolution of DNA Polymerase Families: Evidences for Multiple Gene Exchange Between Cellular and Viral Proteins. **2002**, *54*, 763-773.

39) Borer, P. N. (1975) in Handbook of Biochemistry and Molecular Biology: Nucleic Acids (Fasman, G. D., Ed.) 3rd ed., Vol. 1, p 589, CRC Press, Cleveland, OH.